Fluorogenic NIR-Probes Based on 1,2,4,5-Tetrazine Substituted BF2-Azadipyrromethenes

AUTHOR(S)

Dan Wu, Donal F. O'Shea

ChemComm

Accepted Manuscript

This article can be cited before page numbers have been issued, to do this please use: D. Wu and D. O'Shea, *Chem. Commun.*, 2017, DOI: 10.1039/C7CC06545K.

ROYAL SOCIETY OF CHEMISTRY

rsc.li/chemcomm

ROYAL SOCIETY OF CHEMISTRY View Article Online
DOI: 10.1039/C7CC06545K

Journal Name

COMMUNICATION

Fluorogenic NIR-Probes Based on 1,2,4,5-Tetrazine Substituted BF_2-Azadipyrromethenes

Dan Wu[a] and Donal F. O'Shea[a]

Received 00th January 20xx,
Accepted 00th January 20xx

DOI: 10.1039/x0xx00000x

www.rsc.org/

A series of 1,2,4,5-tetrazine integrated near infrared (NIR) fluorophores based on the BF_2 azadipyrromethene (NIR-AZA) class has been synthesised and their ability to modulate emission from low to high in response to Diels-Alder cycloadditions has been assessed. Substituents on the tetrazine component of the probe (Cl, OMe, *p*-$NO_2C_6H_4O$) were seen to strongly influence quantum yields, fluorescence enhancement factors, and rates of cycloadditions. Cycloadditions between tetrazine-NIR-AZA constructs and a strained alkyne substrate were seen to be highly efficient in organic or aqueous solutions and in gels with high fluorescence enhancements of up to 48-fold observed. Real-time demonstration of the cycloaddition mediated fluorogenic property was achieved by imaging the "turn-on" reaction within a continous flow micro-reactor. Preliminary evidence indicates that excited state quenching involves a photoinduced electron transfer.

Near infrared (NIR) fluorophores continue to attract research attention due to the ever growing need for new agents for use in material, biological and medical applications. Potential uses span from optoelectronic / solar energy materials, to research imaging probes and, to fluorescence guided precision surgery.[1] The BF_2-azadipyrromethene (NIR-AZA) fluorophores are an emerging class of NIR emitters which have grown in popularity due to their relative ease of synthesis which allows for customisation of their properties as needed (Fig. 1).[2] Many NIR-AZA *off* to *on* switching fluorescent probes have been reported, however to date no fluorogenic NIR-AZA probe with a switch on emission in response to a inverse electron demand Diels Alder (IEEDA) reaction has been developed.[3] Two essential components for bio-orthogonal fluorogenic probes are that the reacting component of the probe must effectively quench the fluorophore excited state and the chemical transformation that switches on the emission must be effective under mild, catalyst free, conditions. 1,2,4,5-Tetrazines can satisfy both these criteria as they undergo highly efficient inverse electron demand Diels-Alder (IEDDA) cycloadditions with alkenes and alkynes to produce pyridazines and can act as an excited state quencher of fluorophores.[4] Following the earliest reports of tetrazine fluorogenic probes, their development for use with several fluorophore classes has recently accelerated.[5] The mechanisms of tetrazine mediated excited state quenching most utilised to date are Förster resonance energy transfer (FRET) and through-bond energy transfer (TBET).[6] The requirement of spectral overlap between fluorophore emission and tetrazine absorbance (λ_{max} ~500-550 nm), which would not be present for NIR-emitters such as **1**, excludes the use of FRET as a quenching mechanism. While TBET does not have this requirement, only limited progress has been achieved with probes that emit in the 650 nm range and none has been reported with emissions above 700 nm.[7] As π-deficient tetrazines are known to be good electron acceptors, the potential exists to exploit a photoinduced electron transfer (PET) quenching mechanism for NIR-fluorogenic probes.[8,9]

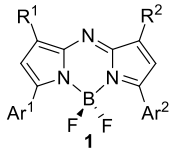

1

Figure 1. General structure of BF_2-azadipyrromethene (NIR-AZA) fluorophores

Herein, we describe the design, synthesis, characterization, and fluorogenic characteristics of three tetrazine-NIR-AZA probes. The previously reported mono-phenolic substituted BF_2-azadipyrromethene **2** was selected as one starting component as it was anticipated that it would undergo nucleophilic substitution reactions with the 3-chloro-tetrazines **3a**-**c** to generate the fluorogenic probes (Scheme 1).[3a] As the efficiency of both IEDDA cycloadditions and fluorophore excited state quenching would be influenced by electronically differing substituents, three example tetrazines were selected for investigation.[4] Reaction of 3,6-dichlorotetrazine **3a**, 3-chloro-6-

[a] *Department of Pharmaceutical and Medicinal Chemistry, Royal College of Surgeons in Ireland, 123 St. Stephen's Green, Dublin 2, Ireland. donalfoshea@rcsi.ie*

Electronic Supplementary Information (ESI) available: experimental data, absorption, emission and NMR spectra, turn-on fluorescence movie, X-ray data]. See DOI: 10.1039/x0xx00000x

methoxy-1,2,4,5-tetrazine **3b** and 3-chloro-6-(4-nitrophenoxy)-1,2,4,5-tetrazine **3c** with **2** provided **4a**-**c** with three electronically differing C-6 tetrazine substituents Cl, MeO, and *p*-$NO_2C_6H_4O$. Commercially available dichlorotetrazine **3a** was used to produce **3b** and **c** by reaction with methanol or *p*-nitrophenol respectively as described in the ESI. Probes **4a**-**c** were readily made, in good yields, at rt in dichloromethane utilising diisopropylethylamine (DIPEA) as base (Scheme 1).

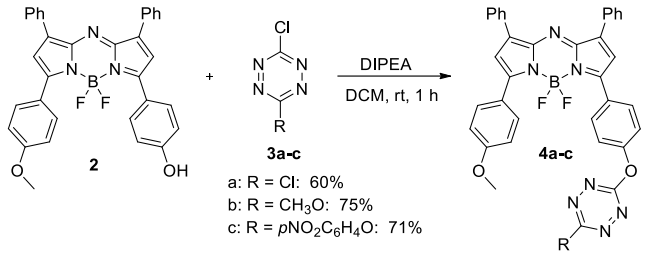

Scheme 1. Synthesis of tetrazine substituted NIR-AZAs **4a**-**c**.

Absorbance and emission spectra of **4a**-**c** in $CHCl_3$ showed similar λ_{max} values at 674±1 nm and 703±1 nm respectively (Table 1). The 12 nm hypsochromic shift in absorbance band upon tetrazine substitution of **2** is indicate of a weak electronic coupling between the tetrazine and the fluorophore. Due to the very low extinction coefficient of the longest wavelength tetrazine bands, they could not be seen in the absorbance spectra of **4a**-**c** (Fig. S1, ESI). Encouragingly, the fluorescence quantum yields measured in $CHCl_3$ of **4a** and **c** were low at 0.007 with the *p*-OMe substituted derivative **4b** marginally higher at 0.05. As the quantum yield of the starting fluorophore **2** is 0.32 this clearly shows that the inclusion of a tetrazine caused excited state quenching with the electron withdrawing Cl and *p*-nitrophenol substituted derivatives being more effective quenchers than the OMe (Table 1).

Table 1 Photophysical properties of **2** and **4a**-**c**[a]

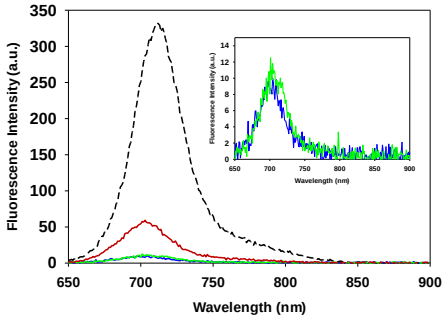

Compound	λ_{max} abs / nm $CHCl_3$ (C_6H_{12})	λ_{max} flu / nm $CHCl_3$ (C_6H_{12})	Φ_{Flu}[b] $CHCl_3$ (C_6H_{12})
2	686 (680)	711 (702)	0.32 (0.33)
4a	673 (670)	702 (694)	0.007 (0.35)
4b	674 (670)	703 (695)	0.05 (0.37)
4c	674 (669)	703 (695)	0.007 (0.34)

[a] In chloroform or cyclohexane at conc = 1×10^{-6} M. [b] Compound **1** R^1/R^2=Ph, Ar^1/Ar^2=*p*-$MeOC_6H_4$ (ϕ=0.36) used as a standard.[11] Black dashed line **2**. Blue line **4a**; red line **4b**; green line **4c**. Inset, expanded view of **4a** and **4c**.

This would be consistent with the electron donating OMe reducing the susceptibility of the tetrazine to act as an electron acceptor. If the quenching mechanism was via a PET then in accord with the Marcus-Jortner model of electron transfer processes it would be expected that this quenching would be thermodynamically less favourable in non-polar solvents such as cyclohexane.[10] This, in fact, was the case with the quantum yields of **4a**-**c** significantly higher in cyclohexane at 0.35, 0.37 and 0.34 respectively and comparable to **2** at 0.33 (Table 1).

A single crystal of **4c**, obtained by the slow evaporation of a chloroform solution, was used for analysis by X-ray crystallography.[12] Comparison of the torsion angles between the four aryl and pyrrole rings showed that the tetrazine substituted position (φ3) had the largest angle of 45.8°, with the others (φ1, φ2, φ4) ranging from 10.3° to 19.8° (Fig. 2). Additionally, the tetrazine ring and the aryl ring linking it to the fluorophore were almost orthogonal to each other with the dihedral angle measured at 67.8°, which positioned the tetrazine ring within 9.1 Å from the centre of the fluorophore, which would be within range for an effective PET (Fig. S2, ESI).[8c]

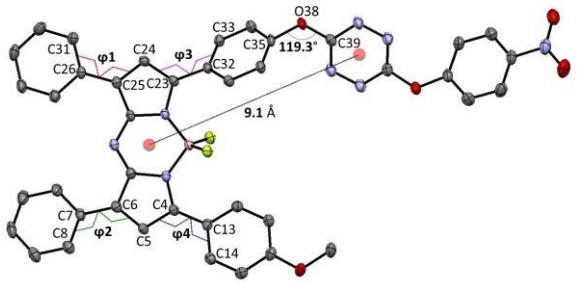

Compound	φ1[°]	φ2[°]	φ3[°]	φ4[°]
4c	10.3(4)	17.2(5)	45.8(4)	19.8(4)

Fig. 2. X-Ray single crystal structure of fluorogenic NIR-AZA **4c.** φ1 (brown) C(24),C(25),C(26),C(31); φ2 (green) C(5),C(6),C(7),C(8); φ3 (purple) C(24),C(23),C(32),C(33); φ4 (blue) C(5),C(4),C(13),C(14).

With the first aim of tetrazine mediated quenching of the NIR-AZA excited state achieved, the next stage was to investigate the potential for turning-on of emission in response to a tetrazine/strained alkyne cycloaddition. (1R,8S,9s)-Bicyclo[6.1.0]non-4-yn-9-ylmethanol (BCN)[13] **5** was chosen as a representative strained alkyne and reactions were first performed in $CDCl_3$ at 21 °C with monitoring by ^{1}H NMR. Encouragingly, each of **4a-c** reacted efficiently with 1.1 equiv. of **5**, with electron withdrawing substituted **4a** and **c** being fastest and electron donating OMe substituted **4b** being slower (Scheme 2). Reaction half-lives were measured as 5.0, 14.9 and 5.2 min for **4a**-**c** respectively, clearly illustrating the effectiveness of the transformation under mild, catalyst free, conditions (Fig. 3, Fig. S3 ESI). Encouragingly, this reactivity trend mirrored the effectiveness of the tetrazines to quench excited states, such that the more effective quenchers reacted faster. When reactions were performed on a larger scale in dichloromethane, yields of isolated products **6a**-**c** were high, ranging from 85-90% following purification.

View Article Online
DOI: 10.1039/C7CC06545K

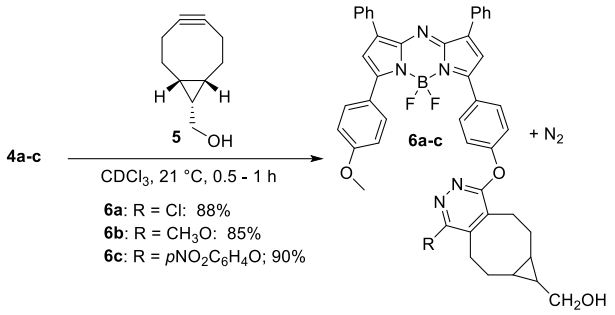

Scheme 2. IEDDA reactions of **4a-c** with **5**.

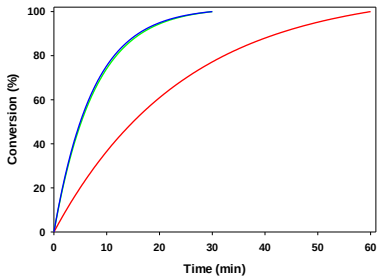

Fig. 3. ^{1}H NMR monitored conversion of **4a-c** with **5** at 21°C. Blue line **4a**; red line **4b**; green line **4c**.

Spectroscopic analysis of **6a-c** in $CHCl_3$ showed significantly increased fluorescence quantum yields of 0.33, 0.34 and 0.34 respectively which were all comparable to the starting fluorophore **2**. Comparison of quantum yields showed that probes **6a** and **6c** both had excellent fluorescence enhancement factors (FEF) of 47 and 48 fold respectively. In contrast, the OMe substituted tetrazine derivative **6b** was less at 7 fold FEF, which is a consequence of the less effective excited state quenching in **4b**. The large FEFs upon IEDDA transformation of **4a** and **c** offers potential for their responsive fluorescence imaging application with good signal to background ratios.

The tetrazine NIR-AZA **4c** was chosen to test its ability to perform as a fluorogenic probe in water. An aqueous solution was readily produced using the surfactants poloxamer 188 and polysorbate 20 with a λ_{max} emission at 715 nm and were shown to be stable by HPLC at 37 °C (Fig. S4 ESI). This aqueous solution was treated with BCN **5** at 37 °C, and the NIR-fluorescence intensity was observed to rapidly increase over time reaching a maximum after 30 min (Fig. 4). Comparison of fluorescence peak area at the start and end of the experiment gave an FEF value of 38. Reaction of **4a** (FEF=46) with **5** was equally effective under these conditions, while **4b** (FEF=17) was comparatively slower, not reaching a maximum intensity until 250 min (Fig. 4, Fig. S5 ESI). As surfactant formulated NIR-AZA fluorophores have been successfully used for intracellular[3a] and tissue imaging[2b] the application of **4a**, **c** as bio-orthogonal fluorogenic probes are wide ranging and currently under development.

To test if the fluorescence switch on IEDDA reaction could proceed within a gel, probe **4c** was embedded within an agarose gel by mixing with the agarose solution prior to gel formation. To date, IEDDA fluorogenic reactions in gels have gone unexplored in spite of their potential for use in gel based diagnostics and biosensing.[14] Panel A of Fig. 5 shows the white light image of the gel, with panel B showing the corresponding NIR-fluorescence image which shows that inclusion of **4c** within the gel has not compromised the excited state quenching as little fluorescence can be observed. After submerging the gel in an aqueous solution of **5** at rt overnight and re-imaging, the gel was seen to be strong NIR-fluorescent as a consequence of the cycloaddition reaction (Fig. 5, panel C).

A key advantage of fluorogenic probes is that they can be utilised for real-time continuous imaging, presuming that the fluorophore when switched on is sufficiently photo-stable and not prone to photo-bleaching. Off to on responsive NIR-AZA

Table 2 Photophysical properties of **6a-c**[a]

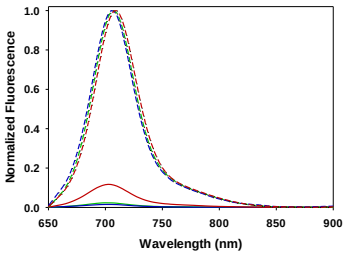

Comp.	λ_{max} abs / nm	Ext. coeff. / $cm^{-1}M^{-1}$	λ_{max} flu / nm	Φ_F[b]	FEF
6a	676	92,000	707	0.33	47
6b	678	91,000	709	0.34	7
6c	677	90,000	708	0.34	48

[a] In $CHCl_3$, conc = 1×10^{-6} M. [b] Compound **1** R^1/R^2=Ph, Ar^1/Ar^2=*p*-$MeOC_6H_4$ (ϕ=0.36) used as a standard.[11] Blue dashed line **6a**; red dashed line **6b;** green dashed line **6c**. Solid blue line **4a**; solid red line **4b**; solid green line **4c**.

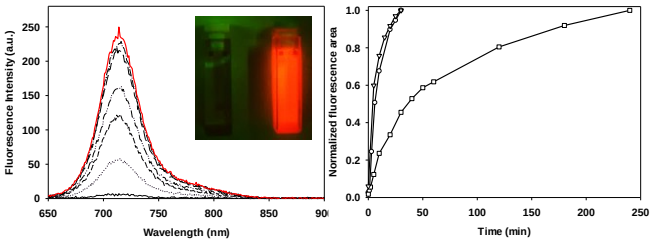

Fig. 4. Left: Turn-on of fluorogenic probe **4c** by **5** (50 equiv) in water at 37 °C (conc.= 0.7×10^{-6} M). See Fig. S5 ESI for data using 10 equiv of **5**. Black solid line: 0 min, red solid line: 30 min. Inset picture: NIR-fluorescence image taken of cuvettes at 0 min (left) and at 30 min (right). Right: Plot of increasing NIR-fluorescence over time for the reactions of **4a-c** with BCN **5** in water at 37 °C, **4a** (triangles), **4b** (squares), **4c** (circles).

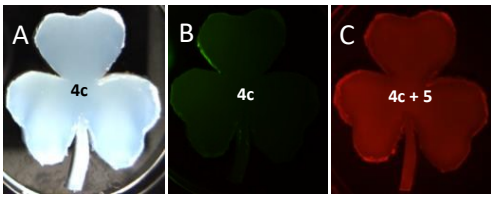

Fig. 5. NIR-fluorescence turn-on of **4c** in agarose gel. A: White light image of shaped gel containing **4c**. B: NIR-fluorescence image of gel containing **4c**. C: NIR-fluorescence image of **4c** treated with **5**. Control images of gel doped with **6c** can be seen in Fig. S6, ESI.

DOI: 10.1039/C7CC06545K

probes have previously been shown to be effective for continuous real-time cellular imaging and have excellent photostability.[3e,11] In this report we selected to demonstrate the first real-time imaging within a continuous flow micro-fluidic glass chip. The apparatus set up consisted of two identical 1 mL chips (1 and 2) linked together in sequence, both of which could be continuously NIR-fluorescence imaged simultaneously (Fig. 6, schematic).[15] Experimentally, probe **4c** alone was pumped into chip 1 and upon exiting this chip entered chip 2. Strained alkyne **5** was simultaneously pumped into chip 2. NIR-fluorescence imaging of both chips together showed that no fluorescence from **4c** within chip 1 was detected but as it entered chip 2 and mixed with **5** an immediate turn on of emission was observable which increased in intensity as the two reagents progressed through chip 2 over time (Fig. 6 and Movie 1 ESI). A flow rate of 0.2 ml/min was used, equating to a residence time of 5 min, again showing the high turn on efficiency of this probe. This rapid turn on with ease of detection would be of significant benefit to high throughput, lab-on-a-chip, screening assays.[16]

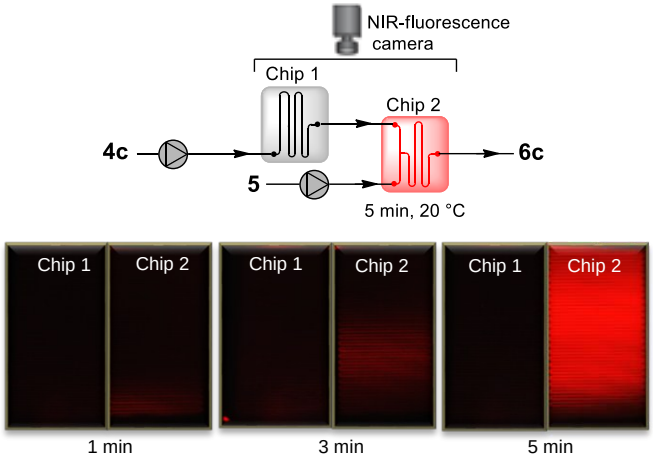

Fig. 6. Real-time continuous imaging of fluorogenic reaction of **4c** with **5** at 20 °C within a continuous flow micro-reactor.

In summary, three closely related tetrazine BF_2-azadipyrromethene fluorophores with varying electron withdrawing and donating substituents at the C-6 position of the tetrazine were successful synthesised. It was found that electron-withdrawing groups at this position were more favourable for excited state quenching and IEDDA alkyne reactions. Preliminary spectroscopic analysis indicate that a PET is involved in excited state quenching which overcomes the lack of spectral overlap between the tetrazine and NIR-AZA components of the probe which is essential for a FRET quenching mechanism. The FEF values upon cycloaddition reaction were high and could be readily recorded and visualised in solution and in gels. Real-time continuous monitoring of the fluorogenic turn-on reaction was demonstrated using a continuous flow micro-reactor apparatus. On-going efforts for this work-program include the translation of these NIR probes for use in material, biological and medical sciences.

DOS gratefully acknowledges Science Foundation Ireland grant number 11/PI/1071(T) for financial support. A patent has been filed on BF_2-azadipyrromethene based NIR fluorophores in which DOS has a financial interest.

Notes and references

1 (a) G. Hong, A.L. Antaris and H. Dai, *Nat. Biomed. Eng.*, 2017, **1**, 0010. (b) V.J. Pansare, S. Hejazi, W.J. Faenza and R.K. Prud'homme, *Chem. Mater.* 2012, **24**, 812. (c) A.L. Vahrmeijer, M. Hutteman, J.R. van der Vorst, C.J.H. van de Velde and J.V. Frangioni, *Nat. Rev. Clin. Oncol.*, 2013, **10**, 507e518.

2 (a) Y. Ge and D. F. O'Shea, *Chem. Soc. Rev.*, 2016, **45**, 3846. (b) H. C. Daly, G. Sampedro, C. Bon, D. Wu, G. Ismail, R. A. Cahill and D. F. O'Shea, *Eur. J. Med. Chem.*, 2017, **135**, 392. (c) D. Wu, S. Cheung, C. J. O'Sullivan, Y. Gao, Z. Chen and D. F. O'Shea, *RSC Adv.*, 2016, **6**, 87373.

3 (a) J. Murtagh, D. O. Frimannsson and D. F. O'Shea, *Org. Lett.*, 2009, **11**, 5386. (b) S. Schutting, T. Jokic, M. Strobl, S. M. Borisov, D. d. Beer and I. Klimant, *J. Mater. Chem. C*, 2015, **3**, 5474. (c) R. E. Gawley, H. Mao, M. M. Haque, J. B. Thorne and J. S. Pharr, *J. Org. Chem.*, 2007, **72**, 2187. (d) M. Gao, R. Wang, F. Yu, J. You and L. Chen, *Analyst*, 2015, **140**, 3766. (e) M. Grossi, M. Morgunova, S. Cheung, D. Scholz, E. Conroy, M. Terrile, A. Panarella, J. C. Simpson, W. M. Gallagher and D. F. O'Shea, *Nat. Commun.*, 2016, **7**, 10855.

4 E. Kozma, O. Demeter, P. Kele, *Chembiochem*, 2017, **18**, 486.

5 (a) N. K. Devaraj, R. Weissleder and S. A. Hilderbrand, *Bioconjugate Chem.*, 2008, **19**, 2297. (b) M. L. Blackman, M. Royzen and J. M. Fox, *J. Am. Chem. Soc.*, 2008, **130**, 13518.

6 For recent examples see: (a) H. X. Wu, S. C. Alexander, S. J. Jin and N. K. Devaraj, *J. Am. Chem. Soc.*, 2016, **138**, 11429. (b) J. J. Gruskos, G. Zhang and D. Buccella, *J. Am. Chem. Soc.*, 2016, **138**, 14639. (c) T. Peng and H. C. Hang, *J. Am. Chem. Soc.*, 2016, **138**, 14423. (d) T. S.-M. Tang, H.-W. Liua and K. K.-W. Lo *Chem. Commun.*, 2017, **53**, 3299. (e) E. Kozma, G. Estrada Girona, G. Paci, E. A. Lemke and P. Kele *Chem. Commun.*, 2017, **53**, 6696.

7 (a) A. Wieczorek, P. Werther, J. Euchner and R. Wombacher, *Chem. Sci.*, 2017, **8**, 1506. (b) N. K. Devaraj, S. Hilderbrand, R. Upadhyay, R. Mazitschek and R. Weissleder, *Angew. Chem. Int. Ed.* 2010, **49**, 2869.

8 (a) G. Clavier and P. Audebert, *Chem. Rev.* 2010, **110**, 3299. (b) Q. Zhou, P. Audebert, G. Clavier, R. Méallet-Renault, F. Miomandre, Z. Shaukat, T.T. Vu and J. Tang, *J. Phys. Chem. C*, 2011, **115**, 21899. (c) A. P. de Silva, T. S. Moody and G. D. Wright, *Analyst*, 2009, **134**, 2385.

9 For examples of BODIPY probes that quench by energy transfer see (a) C. Dumas-Verdes, F. Miomandre, E. Lépicier, O. Galangau, T. T. Vu, G. Clavier, R. Méallet-Renault and P. Audebert, *Eur. J. Org. Chem.*, 2010, 2525. (b) J. C. Carlson, L. G. Meimetis, S. A. Hilderbrand and R. Weissleder, *Angew. Chem., Int. Ed.*, 2013, **52**, 6917.

10 E. E. Neuteboom, S. C. J. Meskers, E. H. A. Beckers, S. Chopin, R. A. J. Janssen, *J. Phys. Chem. A* 2006, **110**, 12363.

11 P. Batat, M. Cantuel, G. Jonusauskas, L. Scarpantonio, A. Palma, D. F. O'Shea and N. D. McClenaghan, *J. Phys. Chem. A*, 2011, **115**, 14034.

12 Data deposited as CCDC 1566927.

13 J. Dommerholt, S. Schmidt, R. Temming, L. J. Hendriks, F. P. Rutjes, J. C. van Hest, D. J. Lefeber, P. Friedl and F. L. van Delft, *Angew. Chem., Int. Ed.*, 2010, **49**, 9422.

14 For related example of membrane assay see; J. Ohata, F. Vohidov and Z. T. Ball, *Mol. BioSyst.* 2015, **11**, 2846.

15 For details of the flow system used see; T. Tricotet and D. F. O'Shea, *Chem. Eur. J.*, 2010, **16**, 6678.

16 G. Du, Q. Fang and J. M. J. den Toonder, *Analytica Chimica Acta*, 2016, **903**, 36.

View Article Online
DOI: 10.1039/C7CC06545K

Graphical abstract

Near infrared fluorogenic probe with tetrazine/alkyne IEDDA cycloaddition switch on in aqueous, gel and micro fluidic systems.